ACTA CHEMICA SCANDINAVICA 22 (1968) 2118–2134

# On the System Ni-Se-Te

ERLING RØST and EGIL VESTERSJØ

*Kjemisk Institutt A, Universitetet i Oslo, Blindern, Oslo 3, Norway*

The ternary system Ni–Se–Te has been studied, mainly by means of X-ray and metallographic methods, and the isothermal section of the phase diagram at 580°C is given. Extended interchangeability of selenium and tellurium was found for all of the phases in the binary systems Ni–Se and Ni–Te at 580°C. A continuous range of solid solution exists between the two phase regions $NiSe_{1.02}$–$NiSe_{1.30}$ and $NiTe_{1.09}$–$NiTe_2$.

A phase existing only in the ternary region has also been found. This phase, which contains between 58 and 59.5 at.–% Ni, has a body centred tetragonal crystal structure, the lattice constants of a sample of proportions $Ni_{.585}Se_{.287}Te_{.128}$ being $a = 7.307$ and $c = 11.55$ Å.

A continuous range of solid solubility appears to exist between the high temperature phases $Ni_{3\pm x}Se_2$ and $Ni_{3\pm x}Te_2$ having *fcc* crystal structure.

A serjes of lattice constants are given for the various phases.

The phase $Ni_3Se_2$ with rhombohedral crystal structure[1–3] undergoes a transformation into a high temperature face centred cubic phase at close to 600°C.[4] Another phase, having the composition $Ni_5Se_6$ and orthorhombic crystal structure, is stable between approximately 400 and 650°C.[4,5] The *B*8 (NiAs)-type structure, which has been reported by several authors, extends from $NiSe_{1.02}$ to $NiSe_{1.30}$ at 550°C,[6] the structure changes from hexagonal to monoclinic symmetry near $NiSe_{1.20}$.[6] The pyrite-type $NiSe_2$ has only a narrow range of homogeneity.[6]

The phase relationships in the binary nickel-tellurium system have recently been discussed by Kok, Wiegers and Jellinek [7] as well as by Barstad, Grønvold, Røst and Vestersjø.[8] A range of solid solubility exists from $NiTe_{0.667}$ to $NiTe_{0.692}$ in samples quenched from 580°C. The crystal structure of this phase is monoclinic in the nickel-rich part, and changes to orthorhombic in the tellurium-rich part of the homogeneity range. According to high temperature X-ray investigations,[7] this phase has a tetragonal structure of the rickardite-type between about 300 and 700°C, while at higher temperatures the structure attains cubic symmetry.[8]

A phase which is richer in tellurium and having orthorhombic crystal structure has also been found.[7,8] According to Kok *et al.*,[7] the composition

of this phase is $NiTe_{0.9}$ whereas Barstad *et al.*[8] determined the composition to be within the range $NiTe_{0.770}$ to $NiTe_{0.775}$. According to Barstad *et al.*[8] the NiAs—$Cd(OH)_2$ (*B*8—*C*6) type homogeneity range extends from $NiTe_{1.09}$ to $NiTe_2$. At 580°C, considerably less than 3 at.—% nickel can be dissolved in liquid tellurium.[8]

## EXPERIMENTAL

The *nickel* metal used in this investigation was obtained by reduction of nickel oxide ("NiO, low in Co and Fe" from The British Drug Houses Ltd.) with dry, oxygen free hydrogen gas. The reduction was carried out at 600°C, after which, the metal was heated for a short period at about 1000°C.

The *selenium* was a gift from Boliden Gruvaktiebolag, Sweden, and bore the analysis (in *ppm*): Na (0.1), As (1.0), S (<0.5) and Cl (<0.5).

The *tellurium* was a 99.999 % pure sample from the American Smelting and Refining Co.

The samples were synthesized by heating appropriate amounts of the elements in evacuated and sealed silica tubes. The samples were first heated to fusion temperature, and after being annealed at 580°C for about three days, were quenched in water. In some cases, the samples were finely ground and reannealed. Preparations with more than 55 at.—% chalcogen were made by adding the required amounts of selenium and tellurium to finely ground samples richer in nickel. Annealing at 580°C for one week was sufficient to achieve equilibrium conditions in these samples.

The alloys were examined by means of metallographic methods, X-ray diffraction and density measurements. X-Ray powder patterns were obtained in a Guinier-type focusing camera, using Cu$K\alpha_1$-radiation ($\lambda = 1.54051$ Å) and KCl ($a = 6.2919$ Å) as calibration standard. High temperature X-ray photographs were obtained using a 19 cm Unicam camera, with the samples sealed in thin-walled silica capillaries. Density measurements were carried out at 25°C by the vacuum pycnometric method.

## PHASE RELATIONSHIPS AT 580°C

Several extended fields of solid solubility exist in the ternary system Ni—Se—Te, and it was found convenient to denote the different phases by capital letters in the following description.

In the nickel-tellurium phase with 58 to 60 at.—% nickel ($NiTe_{0.667}$ to $NiTe_{0.692}$), about 60 % of the tellurium can be substituted with selenium at 580°C (phase *A*). For the phase $Ni_3Se_2$, a more limited interchangeability of selenium with tellurium was observed (phase *B*). Between these two phases, a ternary field (*C*) exists. In $Ni_5Se_6$, nearly 40 % of the selenium can be replaced by tellurium (phase *D*). Extensive exchange of selenium for tellurium is possible also in the phase $NiTe_{0.77}$ (phase *E*). The nickel content of this phase decreases slightly with increasing proportion of selenium. Only an extremely narrow two phase region was found between the phases *D* and *E* at 580°C. The two binary phase regions $NiSe_{1.02}$—$NiSe_{1.30}$ and $NiTe_{1.09}$—$NiTe_2$, with NiAs—$Cd(OH)_2$-type structures, are connected by a broad ternary range of solid solubility (phase *F*), whereas only a limited substitution of tellurium for selenium is possible in the pyrite-type $NiSe_2$ at 580°C (phase *G*).

The extensions of the various phase fields given below refer to the formula $Ni_x(Se_yTe_{1-y})_{1-x}$:

| | | | |
|---|---|---|---|
| *A*: | $0.58 < x < 0.60$; | $0 \leq y < 0.60$ | |
| *B*: | $x = 0.60$; | $0.90 < y \leq 1$ | $(Ni_3(Se_yTe_{1-y})_2)$ |
| *C*: | $0.58 < x < 0.595$; | $0.57 < y < 0.83$ | |
| *D*: | $x = 0.545$; | $0.62 < y \leq 1$ | $(Ni_6(Se_yTe_{1-y})_5)$ |
| *E*: | $0.54 < x < 0.564$; | $0 \leq y < 0.66$ | |
| *F*: | $0.333 < x < 0.495$; | $0 \leq y \leq 1$ | (NiAs–$Cd(OH)_2$ type) |
| *G*: | $x = 0.333$; | $0.94 < y \leq 1$ | $(Ni(Se_yTe_{1-y})_2)$ |
| *H*: | Se–Te liquid phase. | | |

Two and three phase regions are denoted by Roman numerals as follows:

| | | | |
|---|---|---|---|
| I: | $A+Ni$, | XII: | $C+D$, |
| II: | $A+C+Ni$, | XIII: | $B+C+D$, |
| III: | $C+Ni$, | XIV: | $B+D$, |
| IV: | $B+C+Ni$, | XV: | $D+E$, |
| V: | $B+Ni$, | XVI: | $E+F$, |
| VI: | $A+C$, | XVII: | $D+E+F$, |
| VII: | $B+C$, | XVIII: | $D+F$, |
| VIII: | $A+E$, | XIX: | $F+G$, |
| IX: | $A+C+E$, | XX: | $F+H$, |
| X: | $C+E$, | XXI: | $F+G+H$, |
| XI: | $C+D+E$, | XXII: | $G+H$. |

*Table 1.* Compositions of the samples in at.–% and phases present after quenching from 580°C.

| No. | Ni | Se | Te | Phases | No. | Ni | Se | Te | Phases | No. | Ni | Se | Te | Phases |
|---|---|---|---|---|---|---|---|---|---|---|---|---|---|---|
| 1 | 64.0 | 22.0 | 14.0 | Ni+A+C | 39 | 57.9 | 29.1 | 13.0 | C+D | 77 | 53.4 | 32.6 | 14.0 | D+E+F |
| 2 | 64.0 | 23.5 | 12.5 | Ni+A+C | 40 | 57.9 | 35.0 | 7.1 | C+D | 78 | 53.4 | 35.0 | 11.6 | D+F |
| 3 | 64.0 | 26.0 | 10.0 | Ni+C | 41 | 57.5 | 23.5 | 19.0 | A+C+E | 79 | 53.4 | 41.0 | 5.6 | D+F |
| 4 | 64.0 | 31.0 | 5.0 | Ni+B+C | 42 | 57.5 | 25.5 | 17.0 | C+D+E | 80 | 53.0 | 29.0 | 18.0 | E+F |
| 5 | 62.5 | 0.0 | 37.5 | Ni+A | 43 | 57.5 | 37.5 | 5.0 | B+C+D | 81 | 52.0 | 35.0 | 13.0 | D+F |
| 6 | 60.5 | 12.3 | 27.2 | Ni+A | 44 | 57.5 | 40.0 | 2.5 | B+C+D | 82 | 52.0 | 36.0 | 12.0 | D+F |
| 7 | 60.0 | 0.0 | 40.0 | A | 45 | 57.5 | 41.3 | 1.3 | B+D | 83 | 49.5 | 50.5 | 0.0 | F |
| 8 | 60.0 | 2.5 | 37.5 | A | 46 | 56.8 | 0.0 | 43.2 | A+E | 84 | 49.2 | 40.8 | 10.0 | E+F |
| 9 | 60.0 | 5.0 | 35.0 | A | 47 | 56.5 | 6.5 | 37.0 | A+E | 85 | 49.0 | 25.5 | 25.5 | E+F |
| 10 | 60.0 | 6.5 | 33.5 | A | 48 | 56.5 | 13.5 | 30.0 | A+E | 86 | 48.8 | 31.2 | 20.0 | E+F |
| 11 | 60.0 | 10.0 | 30.0 | A | 49 | 56.5 | 21.7 | 21.7 | A+E | 87 | 48.3 | 20.0 | 31.7 | E+F |
| 12 | 60.0 | 20.0 | 20.0 | A | 50 | 56.5 | 25.0 | 18.5 | A+C+E | 88 | 48.1 | 26.0 | 26.0 | F |
| 13 | 60.0 | 23.0 | 17.0 | Ni+A | 51 | 56.5 | 25.6 | 17.9 | C+E | 89 | 48.0 | 10.0 | 42.0 | E+F |
| 14 | 60.0 | 25.0 | 15.0 | Ni+A+C | 52 | 55.7 | 0.0 | 44.4 | E+F | 90 | 47.9 | 0.0 | 52.2 | F |
| 15 | 60.0 | 28.0 | 12.0 | Ni+C | 53 | 55.5 | 3.5 | 41.0 | E | 91 | 44.0 | 28.0 | 28.0 | F |
| 16 | 60.0 | 30.0 | 10.0 | Ni+C | 54 | 55.5 | 6.5 | 38.0 | A+E | 92 | 42.5 | 56.0 | 1.5 | F+G |
| 17 | 60.0 | 33.0 | 7.0 | Ni+C | 55 | 55.5 | 27.2 | 17.4 | C+D+E | 93 | 42.0 | 53.0 | 5.0 | F |
| 18 | 60.0 | 35.0 | 5.0 | Ni+B+C | 56 | 54.7 | 32.0 | 13.3 | D+C | 94 | 40.5 | 54.7 | 4.8 | F+G |
| 19 | 60.0 | 37.5 | 2.5 | B | 57 | 54.6 | 6.5 | 39.0 | E+F | 95 | 40.0 | 30.0 | 30.0 | F |
| 20 | 60.0 | 40.0 | 0.0 | B | 58 | 54.6 | 8.5 | 37.0 | E | 96 | 38.0 | 46.4 | 15.6 | F |
| 21 | 59.5 | 26.1 | 14.4 | A+C | 59 | 54.6 | 10.5 | 35.0 | A+E | 97 | 37.0 | 47.9 | 15.1 | F+G |
| 22 | 59.5 | 28.2 | 12.3 | Ni+C | 60 | 54.6 | 14.0 | 31.5 | A+E | 98 | 36.7 | 31.7 | 31.7 | F |
| 23 | 59.3 | 33.7 | 7.0 | B+C | 61 | 54.6 | 22.7 | 22.7 | E | 99 | 33.3 | 0.0 | 66.7 | F |
| 24 | 59.0 | 28.4 | 12.6 | C | 62 | 54.6 | 25.0 | 20.5 | E | 100 | 33.3 | 20.0 | 46.7 | F |
| 25 | 59.0 | 35.0 | 6.0 | B+C | 63 | 54.6 | 28.0 | 17.5 | E | 101 | 33.3 | 33.3 | 33.3 | F |
| 26 | 58.8 | 0.0 | 41.2 | A+E | 64 | 54.6 | 28.2 | 17.3 | D+E | 102 | 33.3 | 40.0 | 26.7 | F |
| 27 | 58.5 | 6.5 | 35.0 | A | 65 | 54.6 | 30.0 | 15.5 | D | 103 | 33.3 | 45.0 | 21.7 | F+G |
| 28 | 58.5 | 13.0 | 28.5 | A | 66 | 54.6 | 32.9 | 12.6 | D | 104 | 33.3 | 55.0 | 11.7 | F+G |
| 29 | 58.5 | 20.8 | 20.8 | A | 67 | 54.6 | 40.0 | 5.5 | D | 105 | 33.3 | 58.7 | 7.9 | F+G |
| 30 | 58.5 | 25.0 | 16.5 | A+C | 68 | 54.6 | 45.5 | 0.0 | B+D+F | 106 | 33.3 | 62.7 | 4.0 | F+G |
| 31 | 58.5 | 28.7 | 12.8 | C+D | 69 | 54.3 | 30.6 | 15.1 | D+E | 107 | 33.3 | 63.7 | 3.0 | G |
| 32 | 58.0 | 6.5 | 35.5 | A+E | 70 | 54.2 | 22.9 | 22.9 | E | 108 | 33.3 | 64.7 | 2.0 | G |
| 33 | 58.0 | 13.0 | 29.0 | A+E | 71 | 54.2 | 30.0 | 15.8 | D+E | 109 | 33.3 | 66.7 | 0.0 | G |
| 34 | 58.0 | 21.0 | 21.0 | A+E | 72 | 54.2 | 32.2 | 13.6 | D+F | 110 | 30.0 | 35.0 | 35.0 | F+H |
| 35 | 58.0 | 24.4 | 17.6 | A+C | 73 | 54.1 | 30.7 | 15.2 | D+E+F | 111 | 15.0 | 42.5 | 42.5 | F+G+H |
| 36 | 58.0 | 35.0 | 7.0 | B+C | 74 | 53.8 | 10.7 | 35.5 | E+F | 112 | 15.0 | 50.0 | 35.0 | F+G+H |
| 37 | 57.9 | 23.6 | 18.5 | A+C+E | 75 | 53.8 | 23.1 | 23.1 | E+F | 113 | 15.0 | 55.0 | 30.0 | G+H |
| 38 | 57.9 | 25.3 | 16.8 | C+D | 76 | 53.4 | 30.6 | 16.0 | E+F | 114 | 3.0 | 0.0 | 97.0 | F+H |
| | | | | | | | | | | 115 | 3.0 | 97.0 | 0.0 | G+H |

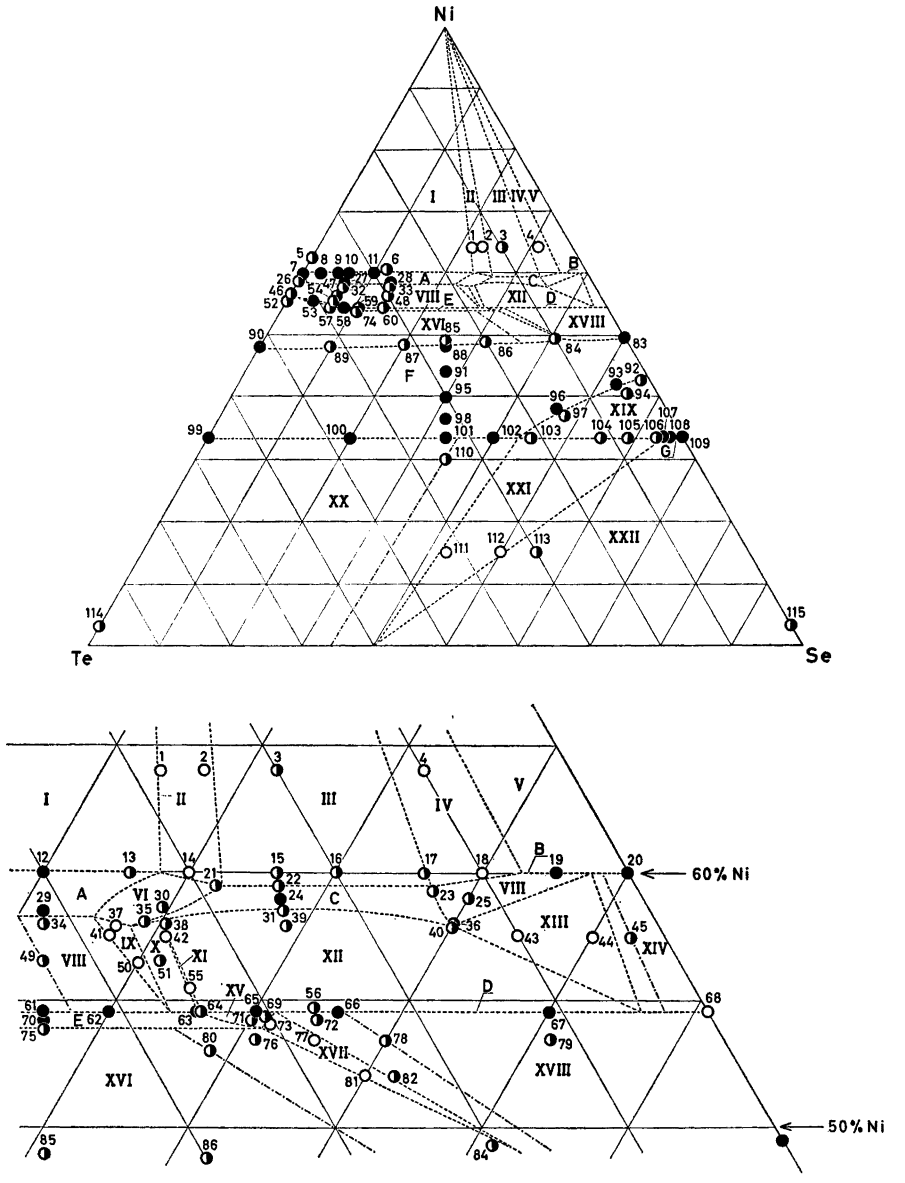


*Fig. 1 a, b.* Ternary plot of alloy composition in at.-%. Filled, half filled and open circles represent one, two and three phases, respectively. The phase boundaries and tie lines limiting the two- and three-phase fields are shown as broken lines, whereas the dotted-broken lines show the tie line direction through some two-phase samples.

The compositions of the synthesized samples, and the phases observed after quenching from 580°C are shown in Table 1. The samples are numbered in order of decreasing nickel fraction, and are represented in the triangular at.—% diagram of Figs. 1 a and b. One-, two-, and three-phase samples are shown as filled, half filled, and open circles, respectively. The phase boundaries of the homogeneity regions, and the tie lines limiting the various two- and three-phase fields, are indicated by broken lines in Figs. 1 a and b.

During the construction of the isothermal section of the ternary phase diagram, tie line directions through some two phase samples (45, 49, 78, 80, and 110) were determined by comparison of lattice constants. These directions are shown by dotted-broken lines in Fig. 1. Estimations of the tie line directions were made on the basis of the following lattice constants:

Sample 45. Phase $B$: $a = 4.241$ Å, $\alpha = 90.73°$
Phase $D$: $a = 3.448$, $b = 11.88$ and $c = 17.08$ Å

Sample 49. Phase $A$: $a = 3.741$ and $c = 5.762$ Å.
Phase $E$: $a = 3.765$ and $c = 12.163$ Å.

Sample 78. Phase $F$: $a = 3.701$ and $c = 5.350$ Å.
Phase $D$: $a = 3.516$, $b = 12.04$ and $c = 17.25$ Å.

Sample 80. Phase $F$: $a = 3.747$ and $c = 5.350$ Å.

Sample 110. Phase $F$: $a = 3.706$ and $c = 5.111$ Å.

The compositions of the various phases in these samples were found by comparing the lattice constants given above with those listed in Table 3 (phase $A$), Table 7 (phase $B$), Table 10 (phase $D$), Table 11 (phase $E$), Table 14 (phase $F$), and Table 15 (phase $F$).

The isothermal section of the phase diagram of the system Ni—Se—Te at 580°C is given in Fig. 2. Single phase fields are shown as shaded areas or heavy lines, two phase fields are indicated by tie lines, and three phase fields by open triangles.

*Table 2.* Lattice constants (Å) at the metal-rich boundary of the phase $A$, $Ni_3(Se_yTe_{1-y})_2$.

| Sample | $y$ | $a$ | $b$ | $c$ | $\beta°$ | Symmetry |
|---|---|---|---|---|---|---|
| 7 | 0.00 | $2\times3.775$ | 3.800 | 6.100 | 91.22 | monoclinic |
| 8 | 0.063 | $2\times3.769$ | 3.793 | 6.084 | 90.78 | » |
| 9 | 0.125 | $2\times3.769$ | 3.791 | 6.006 | 90.27 | » |
| 10 | 0.163 | 3.783 | — | 5.957 | 90.00 | tetragonal |
| 11 | 0.250 | 3.777 | — | 5.890 | 90.00 | » |
| 12 | 0.500 | 3.745 | — | 5.779 | 90.00 | » |
| 13 | 0.575 | 3.732 | — | 5.752 | 90.00 | » |
| 14 | 0.625 | 3.725 | — | 5.744 | 90.00 | » |

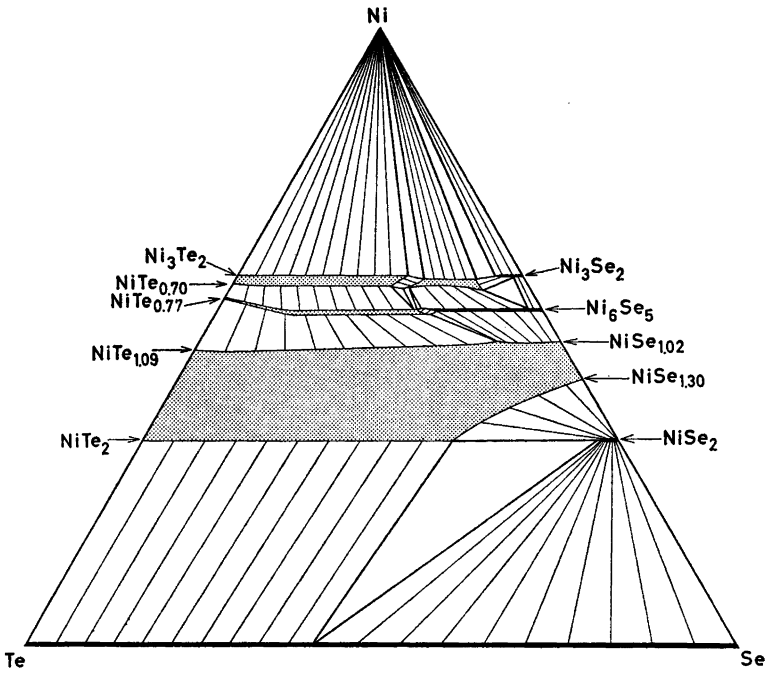


*Fig. 2.* Isothermal section of the Ni—Se—Te phase diagram at 580°C. Single phase fields are shown as heavy lines or shaded areas, two-phase fields are indicated by tie lines and three-phase fields by open triangles.

## DESCRIPTION OF THE PHASES

*Phase A.* A progressive decrease in lattice constants accompanies the gradual replacement of tellurium by selenium in the phase $NiTe_{0.667}$—$NiTe_{0.692}$. In the tellurium-rich region, the tetragonal, high temperature rickardite-type

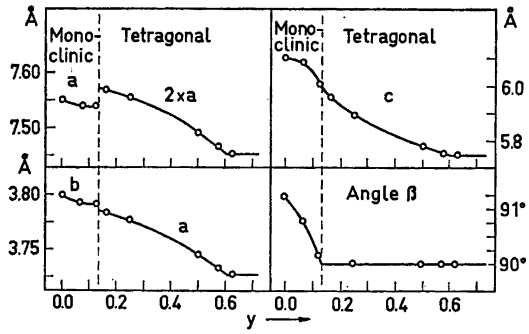


*Fig. 3.* Lattice constants (Å) *versus* Se/Te mole fraction along the metal-rich boundary of phase *A*, $Ni_3(Se_yTe_{1-y})_2$.

*Table 3.* Lattice constants (Å) of phase *A* observed in samples near the chalcogen-rich boundary.

| Sample | Composition | *a* | *b* | *c* | Symmetry |
|---|---|---|---|---|---|
| 26 | $Ni_{.588}Te_{.412}$ | 3.771 | 3.795 | 6.065 | orthorhombic |
| 32 | $Ni_{.580}Se_{.065}Te_{.355}$ | 3.768 | — | 5.963 | tetragonal |
| 33 | $Ni_{.58}S_{.13}eTe_{.29}$ | 3.761 | — | 5.863 | » |
| 34 | $Ni_{.58}Se_{.21}Te_{.21}$ | 3.734 | — | 5.757 | » |
| 37 | $Ni_{.579}Se_{.236}Te_{.185}$ | 3.721 | — | 5.741 | » |

phase [7] appears to be unquenchable, whereas in the selenium-rich preparations of phase *A*, this structure is retained after quenching. Lattice constants of some samples on the nickel-rich phase boundary, $Ni_3(Se_yTe_{1-y})_2$, are listed in Table 2 and plotted in Fig. 3. At a selenium content corresponding to $y=0.13$, the $\beta$-angle reaches 90°, and at the same composition, discontinuous changes in the dimensions of the *a*- and *b*-axes occur, resulting in tetragonal symmetry for samples in the selenium-rich region.

At the chalcogen-rich boundary of phase *A*, the structure changes from orthorhombic to tetragonal symmetry as the selenium fraction increases. Lattice constants are given in Table 3.

The densities of some phase *A* samples were measured, and the results presented in Table 4, together with the calculated number of atoms per unit cell. Within the region of tetragonal structure, the unit cell contains two chalcogen atoms, while a limited variation in the amount of nickel is possible.

The crystal structure of the tetragonal high temperature phase $Ni_{3\pm x}Te_2$ is, according to Kok *et al.*,[7] similar to that of rickardite, $Cu_{2.8}Te_2$, which is intermediate between the *B*10 (PbO)- and *C*38 ($Fe_2As$)-type structures. In order to determine whether the ternary samples of phase *A* possess the same

*Table 4.* Densities and unit cell content of some samples of phase *A*.

| Sample | Composition | Unit cell volume | Density g/cm³ | Atoms per unit cell Ni | Se | Te | Se+Te |
|---|---|---|---|---|---|---|---|
| 7 | $Ni_{.60}Te_{.40}$ | 175.95 | 8.168 | 6.02 | 0.00 | 4.01 | 4.01 |
| 11 | $Ni_{.60}Se_{.10}Te_{.30}$ | 84.01 | 8.030 | 2.99 | 0.50 | 1.50 | 2.00 |
| 12 | $Ni_{.60}Se_{.21}Te_{.21}$ | 81.03 | 7.856 | 3.01 | 1.00 | 1.00 | 2.00 |
| 34 [a] | $Ni_{.58}Se_{.21}Te_{.21}$ | 80.27 | 7.623 | 2.76 | 1.00 | 1.00 | 2.00 |

[a] Two phase sample containing small amount of phase E.

type of structure, parameter refinements were carried out for two samples, $Ni_{.60}Se_{.20}Te_{.20}$ (12) and $Ni_{.58}Se_{.21}Te_{.21}$ (34). Referring to the rickardite-type structure with space group $P4/nmm$, the unit cell content is in accordance with the formula $Ni_{2+x}(Se,Te)_2$ and the atoms are situated as follows:

2(Se+Te) in (*c*): $0,\frac{1}{2},z$; $\frac{1}{2},0,\bar{z}$.
2 Ni in (*a*): $0,0,0$; $\frac{1}{2},\frac{1}{2},0$.
*x* Ni in (*c*): $0,\frac{1}{2},z$; $\frac{1}{2},0,\bar{z}$.

As no superstructure line has been observed on the powder photographs, a mutual statistical distribution of selenium and tellurium was assumed.

Intensities were recorded from Guinier-type powder photographs, and geometric corrections made according to the method given by D'Eye and Wait.[9] The parameters were refined by least-squares methods, the results being those given in Table 5. The reliability factors obtained were 0.092 and 0.058 for samples 12 and 34, respectively. Satisfactory agreement between observed and calculated structure factors was obtained for both samples, as can be judged from the data given in Table 6.

The position parameters given in Table 5 are in reasonably good agreement with those for $Ni_{3\pm x}Te_2$[7] ($z_{Ni}=0.69$ and $z_{Te}=0.29$), and for rickardite, $Cu_{2.8}Te_2$[10] ($z_{Cu}=0.73\pm0.01$ and $z_{Te}=0.285\pm0.005$).

*Phase B.* In the rhombohedral phase $Ni_3(Se_yTe_{1-y})_2$, the maximum tellurium content at 580°C corresponds to $y=0.9$ (approx.), but at higher temperatures, increased solubility of tellurium was observed. Thus even in sample 15 ($y=0.7$), the rhombohedral structure was retained on quenching from 700°C. High temperature X-ray photographs from this sample showed that

*Table 5.* Positional parameters, temperature factors and estimated standard deviations for two samples of phase *A*.

Sample 12, $Ni_{.60}Se_{.20}Te_{.20}$

| Atom | *x* | σ(*x*) | *y* | σ(*y*) | *z* | σ(*z*) | *B* | σ(*B*) |
|---|---|---|---|---|---|---|---|---|
| Ni | 0 | — | 0 | — | 0 | — | 3.7 | 0.8 |
| Ni | 0 | — | 0.500 | — | 0.681 | 0.011 | 4.4 | 1.6 |
| Te+Se | 0 | — | 0.500 | — | 0.289 | 0.002 | 0.8 | 0.5 |

Sample 34, $Ni_{.58}Se_{.21}Te_{.21}$

| Atom | *x* | σ(*x*) | *y* | σ(*y*) | *z* | σ(*z*) | *B* | σ(*B*) |
|---|---|---|---|---|---|---|---|---|
| Ni | 0 | — | 0 | — | 0 | — | 4.2 | 0.5 |
| Ni | 0 | — | 0.500 | — | 0.678 | 0.008 | 3.9 | 1.1 |
| Te+Se | 0 | — | 0.500 | — | 0.289 | 0.002 | 1.7 | 0.3 |

*Table 6.* Observed and calculated structure factors of two samples of phase *C*.

| *h k l* | $Ni_{.60}Se_{.20}Te_{.20}$ | | $Ni_{.58}Se_{.21}Te_{.21}$ | |
|---|---|---|---|---|
| | $\|F_{obs}\|$ | $\|F_{calc}\|$ | $\|F_{obs}\|$ | $\|F_{calc}\|$ |
| 0 0 1 | 43 | 42 | 42 | 44 |
| 1 0 1 | 111 | 101 | 106 | 105 |
| 0 0 2 | 85 | 67 | 67 | 59 |
| 1 1 0 | 113 | 96 | 102 | 86 |
| 1 1 1 | 129 | 123 | 123 | 118 |
| 1 0 2 | 37 | 34 | 38 | 36 |
| 1 1 2 | 169 | 191 | 165 | 178 |
| 0 0 3 | 156 | 172 | 154 | 163 |
| 2 0 0 | 198 | 210 | 192 | 195 |
| 2 0 1 | 26 | 19 | 29 | 20 |
| 1 0 3 | 74 | 78 | 71 | 73 |
| 2 1 1 | 92 | 84 | 80 | 78 |
| 2 0 2 | 64 | 61 | 51 | 51 |
| 1 1 3 | 41 | 44 | 34 | 38 |
| 2 1 2 | 29 | 32 | 28 | 30 |
| 0 0 4 | 89 | 99 | 81 | 88 |
| 1 0 4 | 47 | 63 | 48 | 57 |
| 2 0 3 | 122 | 122 | 110 | 111 |
| 2 2 0 | 174 | 153 | 145 | 136 |
| 2 1 3 | 62 | 65 | 52 | 57 |
| 3 0 1 | 83 | 74 | 72 | 64 |
| 2 2 2 | 49 | 56 | 43 | 45 |
| 3 1 0 | 67 | 71 | 59 | 59 |
| 3 1 1 | 72 | 56 | 57 | 51 |
| 2 0 4 | 72 | 75 | 64 | 63 |
| 3 1 2 | 107 | 107 | 89 | 90 |
| 2 1 4 | 62 | 57 | 50 | 47 |
| 2 2 3 | 94 | 92 | 80 | 79 |

at 700°C the structure is of the face-centred cubic type, but transforms to the rhombohedral type on quenching. No detailed investigation of the transformation temperatures between the rhombohedral and cubic structures was carried out. After prolonged annealing at 580°C, the phase *B* was not found

*Table 7.* Lattice constants (Å) of samples within the phase region *B*, $Ni_3(Se_yTe_{1-y})_2$.

| Sample | *y* | Hexagonal *a* | Hexagonal *c* | Rhombohedral *a* | Rhombohedral α° | Quenching temp. °C |
|---|---|---|---|---|---|---|
| 20 | 1.000 | 6.027 | 7.248 | 4.237 | 90.70 | 580 |
| 19 | 0.937 | 6.054 | 7.269 | 4.253 | 90.74 | 580 |
| 18 [a] | 0.875 | 6.068 | 7.280 | 4.262 | 90.77 | 580 |
| 17 | 0.825 | 6.097 | 7.306 | 4.280 | 90.81 | 700 |
| 15 | 0.700 | 6.143 | 7.346 | 4.310 | 90.89 | 700 |

[a] Three phase sample at 580°C.

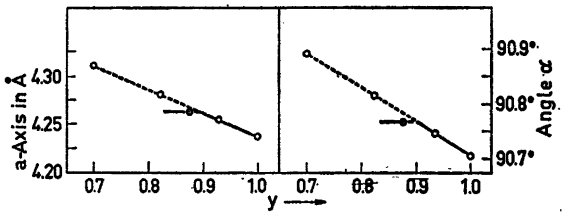


Fig. 4. Lattice constants (Å) *versus* Se/Te mole fraction of phase *B*, $(Ni_3(Se_yTe_{1-y})_2$, with rhombohedral structure. The curve is broken in the region where this phase is unstable at 580°C.

in samples 17 ($y=0.825$) and 15 ($y=0.70$), whereas in sample 18 ($y=0.875$) phase *B* is apparently in equilibrium with Ni and phase *C*.

The lattice constants of the rhombohedral structure as found in samples quenched from 580 or 700°C are given in Table 7, and are plotted *versus* the Se/Te mole fractions in Fig. 4. According to these results, the maximum tellurium content of phase *B* at 580°C corresponds to the composition $Ni_3(Se_{0.9}Te_{0.1})_2$.

*Table 8.* X-Ray powder pattern of sample 31 ($Ni_{.585}Se_{.287}Te_{.128}$) belonging to phase *C*. Cu$K\alpha_1$-radiation.

| $I_{obs}$ | $\sin^2\theta \times 10^5$ | | $h\ k\ l$ |
|---|---|---|---|
| | obs | calc | |
| m | 1549 | 1555 | 1 0 1 |
| w | 1776 | 1777 | 0 0 2 |
| m | 2215 | 2223 | 1 1 0 |
| w | 3995 | 4001 | 1 1 2 |
| m | 5110 | 5113 | 1 0 3 |
| vst | 6217 | 6224 | 2 0 2 |
| m | 7112 | 7114 | 0 0 4 |
| st | 8887 | 8890 | 2 2 0 |
| m | 9341 | 9337 | 1 1 4 |
| m | 9548 | 9558 | 2 1 3 |
| w | 10425 | 10446 | 3 0 1 |
| st | 10669 | 10669 | 2 2 2 |
| w | 11118 | 11113 | 3 1 0 |
| w | 11543 | 11559 | 2 0 4 |
| m | 12234 | 12228 | 1 0 5 |
| m | 12892 | 12891 | 3 1 2 |
| m | 13992 | 14003 | 3 0 3 |
| m | 14886 | 14891 | 3 2 1 |
| m | 15988 | 15981 | 2 2 4 |
| m | 16034 | 16029 | 0 0 6 |
| m | 16686 | 16672 | 2 1 5 |
| st | 17797 | 17780 | 4 0 0 |
| w | 18236 | 18227<br>18229 | 3 1 4<br>1 1 6 |

*Table 9.* Lattice constants (Å), densities and number of atoms per unit cell of samples belonging to phase *C*.[a]

| Sample | Composition | Lattice constants | | Density | Atoms per unit cell | | | |
|---|---|---|---|---|---|---|---|---|
| | | *a* | *c* | g cm$^{-3}$ | Ni | Se | Te | Total |
| 22 | $Ni_{.595}Se_{.282}Te_{.123}$ | 7.305 | 11.540 | 7.443 | 22.52 | 10.67 | 4.66 | 37.85 |
| 31 | $Ni_{.585}Se_{.287}Te_{.128}$ | 7.307 | 11.552 | | | | | |
| 38 | $Ni_{.579}Se_{.253}Te_{.168}$ | 7.340 | 11.596 | 7.563 | 21.95 | 9.59 | 6.37 | 37.91 |
| 40 | $Ni_{.579}Se_{.350}Te_{.071}$ | 7.213 | 11.524 | 7.424 | 21.96 | 13.27 | 2.69 | 37.82 |

[a] These samples are two phase samples containing very small amounts of a second phase in addition to phase *C*.

The densities of samples 15 and 17, which were quenched from 700°C, were found to be 7.486 and 7.356 g cm$^{-3}$, respectively. This corresponds to 2.98 Ni, 1.39 Se, and 0.60 Te atoms per unit cell for sample 15, while for sample 17, the values are 2.97 Ni, 1.63 Se, 0.35 Te atoms. These correspond to the composition $Ni_3(Se_yTe_{1-y})_2$ within the experimental error.

*Phase C.* The powder photographs of the ternary phase *C* could be indexed on the basis of a tetragonal body-centred lattice, and the indexed front X-ray reflections from a sample of this phase are listed in Table 8. Lattice constants, densities and numbers of atoms per unit cell were determined and are presented in Table 9. Within the limits of experimental error, the unit cell is occupied by 38 atoms. The results indicate mutual interchangeability of selenium and tellurium, and also that nickel can to a certain extent replace chalcogen.

The X-ray powder patterns of this phase show a striking similarity to those found for $(Co_xNi_{1-x})_{11}Se_8$ $(0.03<x<0.37)$ by Haraldsen *et al.*[11] This phase probably belongs to one of the space groups, $I4/mmm$, $I\bar{4}2m$, $I4mm$, or $I422$,

*Table 10.* Lattice constants (Å) of phase *D*, $Ni_6(Se_yTe_{1-y})_5$.

| Sample | *y* | *a* | *b* | *c* |
|---|---|---|---|---|
| 64[a] | 0.619 | 3.546 | 12.12 | 17.28 |
| 65 | 0.660 | 3.533 | 12.09 | 17.27 |
| 56[b] | 0.700 | 3.518 | 12.06 | 17.26 |
| 72[b] | 0.700 | 3.517 | 12.05 | 17.25 |
| 66 | 0.722 | 3.516 | 12.03 | 17.24 |
| 67 | 0.880 | 3.471 | 11.94 | 17.15 |
| 68 | 1.000 | 3.439 | 11.87 | 17.05 |

[a] Sample 64 contain very small amounts of phase *E* in addition to the major phase *D*.
[b] The nickel fractions in samples 56 and 72 are somewhat different from that of the other samples.

*Table 11.* Lattice constants (Å) of phase *E*.

| Sample | Composition | *a* | *b* | *c* | Symmetry |
|---|---|---|---|---|---|
| 46 | $Ni_{.568}Te_{.432}$ | 3.912 | 6.872 | 12.38 | orthorhombic |
| 52 | $Ni_{.556}Te_{.444}$ | 3.921 | 6.875 | 12.37 | » |
| 53 | $Ni_{.555}Se_{.035}Te_{.410}$ | 3.896 | 6.839 | 12.34 | » |
| 54 | $Ni_{.555}Se_{.065}Te_{.380}$ | 3.870 | 6.744 | 12.29 | » |
| 57 | $Ni_{.546}Se_{.065}Te_{.390}$ | 3.870 | 6.743 | 12.29 | » |
| 58 | $Ni_{.546}Se_{.085}Te_{.370}$ | 3.833 | | 12.20 | hexagonal |
| 59 | $Ni_{.546}Se_{.105}Te_{.350}$ | 3.823 | | 12.19 | » |
| 60 | $Ni_{.546}Se_{.140}Te_{.315}$ | 3.818 | | 12.18 | » |
| 61 | $Ni_{.546}Se_{.227}Te_{.227}$ | 3.765 | | 12.17 | » |
| 62 | $Ni_{.546}Se_{.250}Te_{.705}$ | 3.758 | | 12.16 | » |
| 63 | $Ni_{.545}Se_{.280}Te_{.175}$ | 3.735 | | 12.14 | » |
| 74 | $Ni_{.538}Se_{.107}Te_{.355}$ | 3.822 | | 12.20 | » |

and the unit cell contains 22 metal and 16 selenium atoms. The same proportion between nickel and chalcogen atoms is found at the chalcogen rich boundary of phase *C* (samples 38 and 40).

*Phase D.* The difficulty of preparing a pure sample of $Ni_6Se_5$ has been mentioned in a previous paper.[11] By partial substitution of tellurium for selenium, however, single phase samples of $Ni_6(Se_yTe_{1-y})_5$ were obtained, and the phase was found to exist in the range corresponding to $0.62<y\leqq 1$ at 580°C. The crystal structure of this phase is orthorhombic with the following extinctions: *hkl* when $h+k=2n+1$, *h0l* when $l=2n+1$. This corresponds to the space groups $Cmc2_1$, $Ama2$, and $Cmcm$. Lattice constants of the phase *C*, which are presented in Table 10, show a smooth increase with increasing tellurium fraction. The densities of the two samples 67 and 65 were determined to be 7.272 and 7.477 g cm$^{-3}$, respectively. These figures correspond to 24.04 Ni, 17.63 Se, and 2.40 Te atoms per unit cell for sample 67, and for sample 65 the values are 23.99, 13.20, and 6.80, respectively. This is in agreement

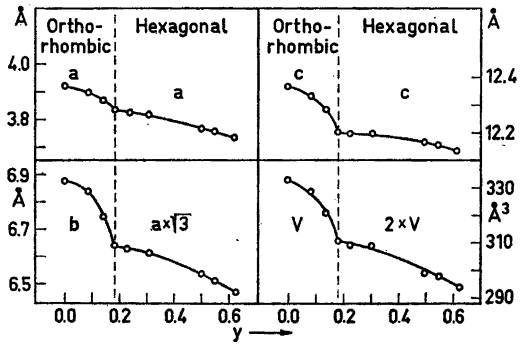


*Fig. 5.* Lattice constants (Å) and unit cell volume (Å$^3$) of phase *E*, $Ni_x(Se_yTe_{1-y})_{1-x}$ *versus* Se/Te mole fraction.

*Table 12.* Densities and number of atoms per unit cell of samples of phase *E*.[a]

| Sample | Composition | Density g cm$^{-3}$ | Atoms per unit cell Ni | Se | Te | Se+Te |
|---|---|---|---|---|---|---|
| [b] | $Ni_{.565}Te_{.435}$ | 8.107 | 10.35 | 0 | 7.97 | 7.97 |
| 60 | $Ni_{.546}Se_{.139}Te_{.315}$ | 7.864 | 4.79 | 1.22 | 2.77 | 3.99 |
| 62 | $Ni_{.546}Se_{.250}Te_{.205}$ | 7.646 | 4.80 | 2.20 | 1.80 | 4.00 |
| 74 | $Ni_{.538}Se_{.107}Te_{.355}$ | 7.965 | 4.67 | 0.93 | 3.08 | 4.01 |

[a] In the calculations, the very small amounts of a second phase present in addition to phase *E* has not been taken into consideration.
[b] Results according to Barstad *et al.*[8]

with the stoichiometric formula $Ni_6(Se_yTe_{1-y})_5$, there being four formula units per unit cell.

*Phase E.* According to Barstad *et al.*[8] a binary nickel-tellurium phase with orthorhombic structure exists in a narrow homogeneity region between $NiTe_{0.77}$ and $NiTe_{0.775}$. When the tellurium is partly substituted with selenium, the nickel fraction of this phase decreases. Lattice constants of phase *E* samples are listed in Table 11, and plotted *versus* composition in Fig. 5. On increasing the selenium fraction, the structure approaches hexagonal symmetry, which is achieved at a composition corresponding to $y=0.18$ according to the formula $Ni_x(Se_yTe_{1-y})_{1-x}$. At this composition, a break can be observed in the curves of Fig. 5. The unit cell volume is halved when the structure changes from orthorhombic to hexagonal symmetry. The results of density measurements, which are presented in Table 12, show that the unit cell contains eight chalcogen atoms in the orthorhombic, and four in the hexagonal regions, whereas a limited variation of nickel content per unit cell is possible.

An indexed powder pattern of a sample from the hexagonal part of phase *E* is given in Table 13.

The limits of the phases *D* and *E* move towards greater tellurium content when the temperature is lowered. This is shown by the presence of phase *D* only in sample 61 ($Ni_{.546}Se_{.227}Te_{.227}$), after cooling slowly to room temperature, whereas the phase *E* was present after quenching from 580°C. Phase *E* was, on the other hand, retained in the slowly cooled sample 60 ($Ni_{.546}Se_{.140}Te_{.315}$).

*Phase F.* Samples in this extended homogeneity range crystallize with a hexagonal structure of the NiAs—$Cd(OH)_2$ type. Only in a narrow region near the selenium-rich part of the binary nickel-selenium system is the structure of phase *F* monoclinic. Lattice constants have been determined for series of samples along the nickel-rich phase boundary, along the chalcogen-rich boundary, and of samples containing equal amounts of selenium and tellurium. The results are to be found in Tables 14, 15, and 16, respectively. Along the metal-rich boundary, the *c*-axis is fairly constant whereas the *a*-axis decreases

*Table 13.* X-Ray data of sample 60, $Ni_{.546}Se_{.140}Te_{.315}$ from the hexagonal part of phase *F*. Cu$K\alpha_1$-radiation.

| $I_{obs}$ | $\sin^2\theta \times 10^5$ obs | $\sin^2\theta \times 10^5$ calc | *h k l* |
|---|---|---|---|
| vw | 1584 | 1592 | 0 0 2 |
| w | 5799 | 5796 | 1 0 1 |
| w— [a] | 5937 | | |
| w+ | 6360 | 6368 | 0 0 4 |
| vst | 7012 | 7020 | 1 0 2 |
| m | 8998 | 9010 | 1 0 3 |
| w— [a] | 10145 | | |
| w | 11791 | 11796 | 1 0 4 |
| st | 15372 | 15379 | 1 0 5 |
| st | 16284 | 16284 | 1 1 0 |
| w— [a] | 16794 | | |
| w | 19761 | 19757 | 1 0 6 |
| vw | 22104 | 22110 | 2 0 1 |
| m— | 22660 | 22652 | 1 1 4 |
| w+ | 23307 | 23304 | 2 0 2 |
| w | 24937 | 24932 | 1 0 7 |
| w | 25294 | 25294 | 2 0 3 |
| w | 25474 | 25474 | 0 0 8 |
| w | 28089 | 28086 | 2 0 4 |
| w+ | 31663 | 31663 | 2 0 5 |

[a] Reflections from phase *A*.

considerably with increasing selenium fraction. At the chalcogen-rich boundary, both the *a*- and *c*-axes decrease with increasing substitution of selenium for tellurium. The maximum selenium fraction at the chalcogen-rich boundary. $Ni(Se_yTe_{1-y})_2$, corresponds to $y=0.64$. This value was determined by comparison of the lattice constants measured in the two-phase samples 103 and 104, with those of the single-phase samples of the $Cd(OH)_2$-type structure (Table 15).

The densities of three samples with one-to-one Se:Te ratio were determined, and the results are tabulated in Table 16. In all of these samples, the unit

*Table 14.* Lattice constants (Å) along the nickel-rich boundary of phase *F*.

| Sample | Composition | *a* | *c* |
|---|---|---|---|
| 90 | $Ni_{.479}Te_{.522}$ | 3.969 | 5.358 |
| 89 | $Ni_{.480}Se_{.100}Te_{.420}$ | 3.909 | 5.350 |
| 87 | $Ni_{.483}Se_{.200}Te_{.317}$ | 3.854 | 5.350 |
| 85 | $Ni_{.490}Se_{.255}Te_{.255}$ | 3.822 | 5.350 |
| 86 | $Ni_{.488}Se_{.312}Te_{.200}$ | 3.784 | 5.350 |
| 84 | $Ni_{.492}Se_{.408}Te_{.100}$ | 3.722 | 5.350 |
| 83 | $Ni_{.495}Se_{.505}$ | 3.661 | 5.356 |

*Table 15.* Lattice constants (Å) along the chalcogene-rich boundary of phase *F*, $Ni(Se_yTe_{1-y})_2$.

| Sample | $y$ | $a$ | $c$ |
|---|---|---|---|
| 99 | 0.000 | 3.857 | 5.267 |
| 100 | 0.300 | 3.771 | 5.205 |
| 101 | 0.500 | 3.716 | 5.139 |
| 102 | 0.600 | 3.685 | 5.088 |
| 103 [a] | 0.675 | 3.677 | 5.071 |
| 104 [a] | 0.825 | 3.677 | 5.071 |

[a] Two phase samples containing phase *F* and *G*.

cells contain two chalcogen atoms, whereas nickel atoms are subtracted from the lattice when the chalcogen fraction increases.

In the binary nickel-selenium system, the crystal structure of phase *F* is monoclinic between $NiSe_{1.20}$ and the selenium-rich phase limit $NiSe_{1.30}$.[6] The structure changes to hexagonal symmetry again on the addition of relatively small amounts of tellurium. Thus, hexagonal crystal structure was found for sample 93 ($Ni_{.42}Se_{.53}Te_{.05}$) but for sample 92 ($Ni_{.425}Se_{.560}Te_{.015}$) the structure is monoclinic.

*Phase G. Pyrite* (C6) *type structure.* In the cubic, pyrite-type structure $NiSe_2$, a limited substitution of tellurium for selenium is possible. The maximum tellurium fraction at 580°C corresponds to $Ni(Se_yTe_{1-y})_2$ with $y=0.94$, which is close to the composition of sample 106. Lattice constants of some samples in this region are given in Table 17.

*The nickel-rich high temperature phase with* fcc *structure.* A series of nickel-rich ternary samples were found to crystallize with face centred cubic structure at high temperatures, and the existence of a continuous homogeneity range from $Ni_{3\pm x}Se_2$ to $Ni_{3\pm x}Te_2$ seems probable. This phase is unquenchable, and investigations were therefore carried out mainly by means of high temperature X-ray diffraction. In addition, differences were observable by means

*Table 16.* Lattice constants (Å), density and unit cell content of $Ni_x(Se_{.5}Te_{.5})_{1-x}$ (Phase *F*).

| Sample | $x$ | Lattice constants | | Density | Atoms per unit cell | | |
|---|---|---|---|---|---|---|---|
| | | $a$ | $c$ | g cm$^{-3}$ | Ni | Se | Te |
| 85 | 0.499 | 3.828 | 5.350 | | | | |
| 88 | 0.481 | 3.822 | 5.350 | 7.729 | 1.84 | 1.00 | 1.00 |
| 91 | 0.440 | 3.791 | 5.332 | | | | |
| 95 | 0.400 | 3.746 | 5.263 | 7.515 | 1.34 | 1.00 | 1.00 |
| 98 | 0.367 | 3.728 | 5.157 | | | | |
| 101 | 0.333 | 3.716 | 5.139 | 7.172 | 1.00 | 1.00 | 1.00 |
| 110 | 0.300 | 3.706 | 5.111 | | | | |

*Table 17.* Lattice constants (Å) of phase *G*, $Ni(Se_yTe_{1-y})_2$ with pyrite-type structure.

| Sample | $y$ | $a$ |
|---|---|---|
| 105 [a] | 0.880 | 5.987 |
| 106 [a] | 0.940 | 5.987 |
| 107 | 0.955 | 5.981 |
| 108 | 0.970 | 5.975 |
| 109 | 1.000 | 5.963 |

[a] Two phase samples.

*Table 18.* Lattice constants (Å) of the *fcc* high temperature phase determined by high temperature X-ray measurements.

| Sample | Composition | $a$ | Temp.°C |
|---|---|---|---|
| 7 [a] | $Ni_{.60}Te_{.40}$ | 5.76 | 900 |
| 12 | $Ni_{.60}Se_{.20}Te_{.20}$ | 5.55 | 700 |
| 15 | $Ni_{.60}Se_{.28}Te_{.12}$ | 5.48 | 700 |
| 19 | $Ni_{.60}Se_{.30}Te_{.10}$ | 5.44 | 590 |
| 20 [b] | $Ni_{.60}Se_{.40}$ | 5.42 | 620 |
| 24 | $Ni_{.590}Se_{.284}Te_{.126}$ | 5.48 | 675 |
| 28 | $Ni_{.585}Se_{.130}Te_{.285}$ | 5.63 | 675 |
| 48 | $Ni_{.565}Se_{.135}Te_{.300}$ | 5.61 | 700 |

[a] Result taken from Barstad *et al.*[8]
[b] Result from Grønvold *et al.*[14]

of metallographic methods between samples quenched from the temperature range of the *fcc* structure and those quenched from lower temperatures. The lattice constants of samples with this structure are given in Table 18. A progressive increase in the lattice dimensions takes place from $Ni_3Se_2$ to $Ni_3Te_2$. A considerable variation in the nickel fraction is possible in the ternary region, analogous to what was found for the binary phase $Ni_{3\pm x}Se_2$. Even sample 48 (56.5 at.— % Ni) is of this phase at 700°C, whereas sample 60 (54.5 at.— % Ni) contains phase *E* in addition to the *fcc* phase at 700°C. Further studies of this high temperature phase are in progress.

*Acknowledgement.* The authors wish to express their appreciation to Professor Haakon Haraldsen for his encouragement and interest in this investigation.

## REFERENCES

1. Jacobsen, E. *Thesis*, University of Oslo (1954).
2. Agarwala, R. P. and Sinha, A. P. B. *Z. anorg. allgem. Chem.* **289** (1957) 203.
3. Hiller, J.-E. and Wegener, W. *Neues Jahrb. Mineral.* **94** (1960) 1147.
4. Grønvold, F., Møllerud, R. and Røst, E. *Acta Chem. Scand.* **20** (1966) 1997.

5. Kuznecov, V. G., Eliseev, A. A., Špak, Z. S., Palkina, K. K., Sokolova, M. A. and Dmitriev, A. V. *Vopr. Met. i Fiz. Poluprov. Akad. Nauk SSSR, Tr. 4-go Soveshch.* **1961** 159.
6. Grønvold, F. and Jacobsen, E. *Acta Chem. Scand.* **10** (1956) 1440.
7. Kok, R. B., Wiegers, G. A. and Jellinek, F. *Rec. Trav. Chim.* **84** (1965) 1585.
8. Barstad, J., Grønvold, F., Røst, E. and Vestersjø, E. *Acta Chem. Scand.* **20** (1966) 2865.
9. D'Eye, R. W. M. and Wait, M. A. *X-Ray Powder Photography in Inorganic Chemistry*, Butterworth's Science Publications (1960) 64.
10. Forman, S. A. and Peacock, M. A. *Am. Mineralogist* **34** (1949) 441.
11. Haraldsen, H., Møllerud, R. and Røst, E. *Acta Chem. Scand.* **21** (1967) 1727.

Received February 7, 1968.